An Energy-Efficient, Inexpensive, Spinal Cord Stimulator with Adaptive Voltage Compliance for Freely Moving Rats

Olafsdottir, Gudrun Erla ; Serdijn, Wouter A.; Giagka, Vasiliki

Citation (APA)
Olafsdottir, G. E., Serdijn, W. A., & Giagka, V. (2018). An Energy-Efficient, Inexpensive, Spinal Cord Stimulator with Adaptive Voltage Compliance for Freely Moving Rats. In *2018 40th Annual International Conference of the IEEE Engineering in Medicine and Biology Society (EMBC): Proceedings* (pp. 2937-2940). Article 8512904 IEEE. https://doi.org/10.1109/EMBC.2018.8512904

Important note
To cite this publication, please use the final published version (if applicable).
Please check the document version above.

An Energy-Efficient, Inexpensive, Spinal Cord Stimulator with Adaptive Voltage Compliance for Freely Moving Rats

Gudrun Erla Olafsdottir, Wouter A. Serdijn and Vasiliki Giagka

Abstract— This paper presents the design and fabrication of an implantable control unit intended for epidural spinal cord stimulation (ESCS) in rats. The device offers full programmability over stimulation parameters and delivers a constant current to an electrode array to be located within the spinal canal. It implements an adaptive voltage compliance in order to reduce the unnecessary power dissipation often experienced in current-controlled stimulation (CCS) devices. The compliance is provided by an adjustable boost converter that offers a voltage output in the range of 6.24 V to 28 V, allowing the device to deliver currents up to 1 mA through loads up to 25 kΩ. The system has been fabricated using discrete components, paving the way to an inexpensive product that can easily be manufactured and batch produced. The control unit occupies a total volume of ~13.5 cm^3 and therefore fulfills the size restrictions of a system to be implanted in a rat. Results indicate that by adjusting the voltage compliance a total power efficiency up to 35.5% can be achieved, saving around 60 mW when using lower stimulation currents or operating on smaller impedances. The achieved efficiency is the highest compared to similar state-of-the-art systems.

I. INTRODUCTION

After spinal cord injury (SCI) the neural pathway within the spinal cord can remain ruptured, often resulting in paralysis. Recently, electrical stimulation of the epidural spinal cord (ESCS) has been shown to facilitate locomotion recovery in SCI rats and humans [1]. Nonetheless, the exact mechanism behind the procedure is not yet fully understood nor optimized. Further animal experiments need to be conducted in which the effects of different stimulation parameters are investigated, on more than one spinal segment. Such experiments are currently hindered by the lack of available technology with the required versatility [2]. Most reported systems for ESCS do not offer multiple site access [3]. The few that are designed to support this feature often suffer from low voltage compliance, i.e., high voltages are required to ensure proper delivery of the stimulation current through high-impedance loads, or still rely on receiving their power from a tethered setup [4] and hence are not suitable for experiments during the animal's natural gait.

We have previously presented a system intended for ESCS capable of delivering fully-programmable, current-controlled stimulation (CCS) pulses (up to 1 mA, with a 25 V output

Gudrun Erla Olafsdottir was with the Bioelectronics Section, Department of Microelectronics, Faculty of Electrical Engineering, Mathematics and Computer Science, Delft University of Technology, Delft, The Netherlands. She is now with the Product Innovation team, Research and Development, Össur hf., Reykjavík, Iceland. (e-mail: golafsdottir@ossur.com).

Wouter A. Serdijn and Vasiliki Giagka are with the Bioelectronics Section, Department of Microelectronics, Faculty of Electrical Engineering, Mathematics and Computer Science, Delft University of Technology, Delft, The Netherlands. (e-mail: w.a.serdijn@tudelft.nl and v.giagka@tudelft.nl).

compliance), to 12 sites on the spinal cord, in any configuration [2] and [5]. Up to 5 different stimulation patterns can be delivered in a time-interleaved fashion. That system comprises an active electrode array and an external control unit responsible for generating a constant current as well as stimulation data for the electrode array. To study ESCS in unrestricted animals a smaller and energy efficient control unit is required, which would fit into a fully implantable system.

A large variety of fully implantable research-oriented stimulating systems for different applications have already been reported [6]–[14]. Most of these use a CCS procedure because of the accurate charge control that it offers, but only two provide full programmability in combination with a high voltage compliance [11] and [14]. The latter two suffer from a reduced power efficiency when either lower stimulation currents are used or the electrode/tissue impedance is less than the maximum expected, as they are driven from fixed voltage supplies. Exploiting the freedom that integrated circuit design offers, some groups have reported a dynamic adjustment of the voltage compliance to increase the efficiency of CCS [15], [16]. To the authors best knowledge this concept has never been implemented using discrete components. Such an implementation can be inexpensive and easily manufactured even by small neuroscience labs, but is challenging due to restrictions posed by off-the-shelf component availability, mismatch and size.

This paper presents the first implantable control unit able to operate from an adaptive voltage supply realized using only discrete components. The new control unit senses the required voltage compliance and uses this feedback to adjust the high voltage supply of the output stage, achieving an overall power efficiency as high as 35.5% and displaying the best efficiency compared to state-of-the-art devices. The rest of this paper explains the system design, and presents and discusses results and design choices.

II. DESIGN

Fig. 1 illustrates a block diagram of the proposed control unit, including the schematics of individual system blocks. Before the experiment, the complete system is connected to a PC via USB, and the user can use a dedicated graphical user interface (GUI) to program desired stimulation patterns and parameters on a microcontroller (MCU) on the control unit. Once the experiment is initiated, the system can be disconnected from the PC so that animals remain untethered. During this time the device is powered by a 6 V battery. Before initiating the selected stimulation paradigm
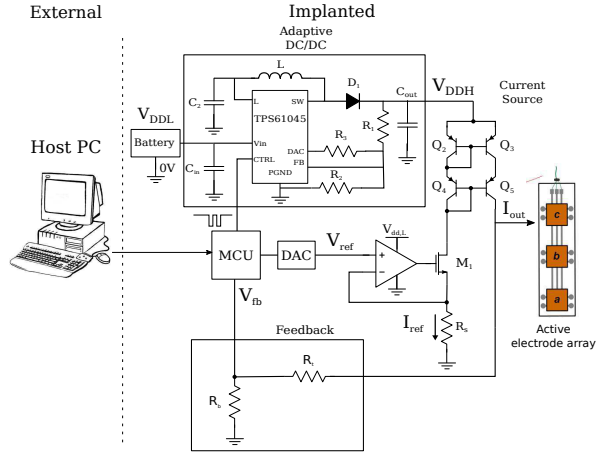
Fig. 1. A block diagram of the proposed system including schematic configurations for different system blocks
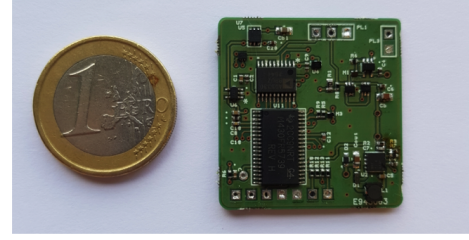

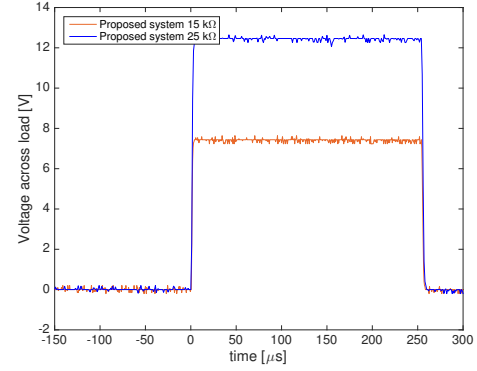Fig. 2. A fabricated version of the proposed system with a one euro coin as a visual size reference

Fig. 3. The measured output waveform of the control unit for different loads and a stimulation current of $500\mu A$

an adaptive DC/DC converter adjusts the voltage compliance slightly above the maximum required to reduce unnecessary power consumption. That voltage value depends on both the electrode/tissue impedance and the programmed stimulation amplitude. This is done via the following procedure: the MCU generates a test pulse, according to the programmed setting intended for stimulation. The maximum voltage appearing at the output of the unit is scaled via the feedback path and fed back to the MCU, sampled via its analog to digital converter (ADC), and used to adjust the output of the adaptive DC/DC converter 1.75 V above the sampled value.

A. Current Source

The unit outputs a rectangular current pulse of a constant but a programmable amplitude up to 1 mA with 10 μA resolution. The CS has been designed for low headroom voltage, low quiescent power and a minimum amount of components, while focusing on speed and accuracy.

The chosen configuration employs an NMOS transistor (M_1) in combination with a feedback resistor, an operational amplifier (op-amp) and a cascoded current mirror. The stimulation current, I_{out}, is generated by programming the output voltage, V_{ref}, of a digital to analog converter (DAC) and connecting it to the positive input terminal of the op-amp, which, in turn, ensures that V_{ref} appears across the source resistor. The current mirror is responsible for copying I_{ref} to the output and increasing the output impedance of the configuration. For accurate copying, the current mirror transistors need to be well matched.

This topology requires a maximum of 0.96 V headroom and can generate a programmable current of 4 μA-1.04 mA.

B. Adaptive Voltage Compliance

Due to specifications from [2], the voltage at the output of the control unit can vary between 2.3 V and 27.3 V, dependent on the electrode-tissue impedance. Since the batteries provide only 6 V, the system needs to include a boost converter. The TPS61045 commercial boost converter can provide an adjustable output voltage up to 28 V by programming an internal 6-bit DAC through a serial control interface, using a pulse-width-modulated (PWM) signal generated by the MCU, and connecting its output to the external feedback loop of the converter. The converter draws only 40 μA of current during operation, and exhibits a high conversion efficiency for the current range of interest.

III. MEASUREMENT RESULTS

Fig. 2 shows the fabricated PCB with a one euro coin for visual size reference. It occupies a total volume of approx. 13.5 cm^3 with the batteries mounted on the bottom side. A similarly sized device has previously been shown to be implantable in a rat [7]. Although the PCB is capable of operating from a battery, all measurements were performed with an external 6 V power supply and conducted using purely resistive loads at the output of the control unit.

A. Output Waveform and Accuracy

Fig. 3 illustrates the waveform of the output current captured on an oscilloscope and plotted by importing the data into Matlab. The accuracy of the system (for programmed currents of 50 μA - 1 mA, in steps of 50 μA) ranges between 99.13% and 96.15%, with a mean value of 97.48%.

B. Adaptive Compliance

To evaluate the functionality of the adaptive compliance, voltage measurements were acquired for multiple loads (between 10 kΩ and 25 kΩ in steps of 2 kΩ) at specific stimulation amplitudes. Fig. 4 illustrates how the compliance adapts to the required voltage measured across the load.
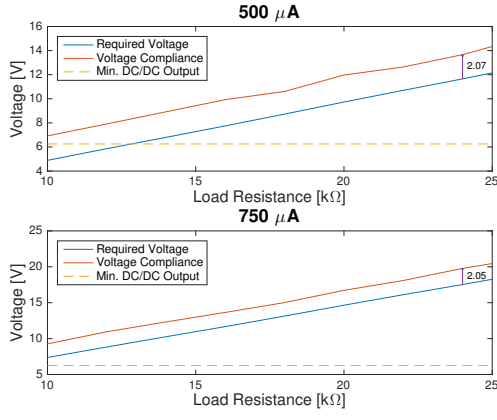
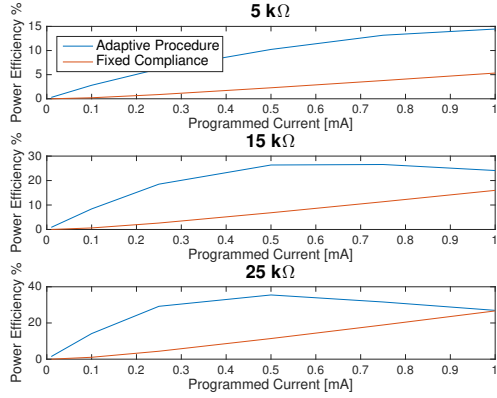Fig. 4. Adjustment of the voltage compliance as a function of load impedance for different current amplitudes

Fig. 5. Power efficiency of the proposed system with an adaptive supply compared to a fixed compliance value

C. Power Efficiency

The maximum power consumption of the system occurs under maximum loading conditions and was measured to be 89.7 mW. At smaller loads or lower stimulation amplitudes the consumption of the unit is reduced even further due to the adaptive compliance. Fig. 5 shows the power efficiency of the system compared to a fixed supply configuration. The graph illustrates the ratio of the power that is delivered to the load over the total input power, in percentages.

IV. DISCUSSION

The waveform of Fig. 3 exhibits a very accurate rectangular pulse with a short response time. Furthermore, it does not exhibit any current spikes that are a common problem for high compliance devices when operating on smaller loads.

Although the proposed topology focused on maximizing the accuracy, some inaccuracies were expected to occur. More specifically, a finite output impedance results in load dependencies, component tolerances contribute to the overall error and the input impedance of the feedback network causes an error of approximately 0.5%. The biggest contribution is however due to the current mirror. Originally the configuration implemented PMOS transistors, but due to the unavailability of suitable off-the-shelf components PNP

transistors were chosen instead. Although matched devices were selected, the mismatch between PNP transistors was up to 2%. Furthermore, the inherent behavior of BJT devices causes a part of the generated current to flow through the base of the transistor and cause an error in the output current. Because of the above, and only at higher amplitudes, errors could become higher than the 10 μA resolution. In any case however, the relative error remains small, in the order of 2.5%, across the entire current range. By either changing the configuration to a Modified Wilson current mirror or implementing matched PMOS devices this error could be reduced further to $\sim$0.5%.

The adaptive procedure offers 64 voltage steps with a possible resolution of 340 mV, which is not fully exploited in this implementation, as, as illustrated in Fig. 4, the output of the converter is, on average, around 2 V higher than the required output voltage. This is to account for CS headroom and potential measurement errors of the feedback network. Decreasing the error would enable the system to make full use of its small step size and further increasing its efficiency.

According to Fig. 5, the maximum efficiency of the system occurs at medium-to-high current amplitudes and small-to-medium loads. This is because under those conditions the power delivered to the load has become significant compared to the quiescent power consumption of the system but does not yet require the maximum voltage compliance. As an example, the maximum power efficiency of 35.5% occurs at a stimulation amplitude of 500 μA and a load of 25 kΩ. Under the same conditions, the power efficiency of a fixed compliance would be only 11.4%. Implementing an adaptive procedure therefore increases the efficiency greatly.

Because of the large variety of system attributes, it is complicated to compare the efficiency of devices reported in literature to the proposed system. Fig. 6 aims to do so by showing an estimated efficiency for state-of-the-art devices at different output currents. Since low-compliant devices, $\leq$ 5 V, are not comparable to the proposed system due to their large differences, these were grouped together. The efficiency of each device within the group was calculated at their specific current amplitude or, in the case of a programmable current, at the middle of the range. The efficency of high-voltage devices was calculated using their lowest, medium and highest specified current and by either assuming a load with an impedance value at the middle of the expected range ([11] and [14]) or, when no range is reported, at the value measured in vivo [9]. The efficiency is calculated as the ratio of the power delivered to the load and the total power provided by the compliance. The proposed system achieves the best power efficiency compared to other devices.

Table I sums up the main attributes of the proposed system and other high compliant devices. Although most of them provide a fully-programmable stimulation current in a similar range, the proposed system has the highest voltage compliance and is the only device with adaptive capabilities.

Currently, the fabricated version occupies a space of approx. 13.5 cm^3, but by selecting a smaller MCU package and reducing the empty space between components it has the

TABLE I

|	Harnack et al. (2008)	Ethier et al. (2011)	Ewing et al. (2013)	This work
Application	DBS	Visual prosthesis	DBS	Epidural spinal cord stimulation
Current amplitude	50 μA – 600 μA, (50 μA resolution)	2.8 μA – 199 μA	13 μA – 1 mA	10 μA – 1 mA
Compliance	18 V Fixed	13.6 V Fixed	20 V Fixed	6.25 V - 28 V Adjustable
Expected impedance	20 kΩ	max. 100 kΩ	12 kΩ	up to 25kΩ
Programmable	Programmable amplitude, frequency and duration are fixed	Fully-programmable	Fully-programmable	Fully-programmable
Size	6 cm^2	9.4 mm^2	4 cm^3	13.5 cm^3
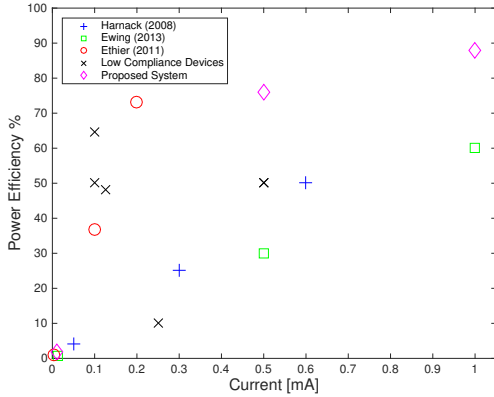
Fig. 6. Power efficiency comparison of reported CCS devices and the proposed system

potential of becoming even smaller. One of the drawbacks is that stimulation parameters cannot be changed dynamically during the experiment. Future work should focus on implementing a wireless communication link that could perhaps also provide power to the implant.

V. CONCLUSION

This paper presented a new, inexpensive, small, implantable, battery-operated electrical stimulation control unit intended for ESCS in freely moving rats, in combination with previously designed electrode arrays [2]. Its design, based on discrete components, implements a novel approach based on adaptive high (up to 28 V) voltage compliance to enhance the power efficiency of CCS devices up to 35.5%, which is the highest compared to similar state-of-the-art systems), while achieving a mean accuracy of 97.48%, and a rectangular pulse with fast response time and no spikes.

ACKNOWLEDGMENTS

REFERENCES

[1] G. Courtine, Y. Gerasimenko, R. van den Brand, A. Yew, P. Musienko, H. Zhong, B. Song, Y. Ao, R. M. Ichiyama, I. Lavrov, R. R. Roy, M. V. Sofroniew, and V. R. Edgerton, "Transformation of nonfunctional spinal circuits into functional states after the loss of brain input," *Nat. Neurosci.*, vol. 12, p. 1333, sep 2009.

[2] V. Giagka, A. Demosthenous, and N. Donaldson, "Flexible active electrode arrays with asics that fit inside the rat's spinal canal," *Biomed. Microdevices*, vol. 17, no. 6, pp. 106–118, Dec 2015.

[3] Q. Xu, D. Hu, B. Duan, and J. He, "A fully implantable stimulator with wireless power and data transmission for experimental investigation of epidural spinal cord stimulation," *IEEE Trans. Neural. Syst. Rehabil. Eng.*, vol. 23, no. 4, pp. 683–692, July 2015.

[4] P. Gad, J. Choe, M. S. Nandra, H. Zhong, R. R. Roy, Y.-C. Tai, and V. R. Edgerton, "Development of a multi-electrode array for spinal cord epidural stimulation to facilitate stepping and standing after a complete spinal cord injury in adult rats." *J. Neuroeng. Rehabil.*, vol. 21, pp. 10–12, 2013.

[5] V. Giagka and A. Demosthenous, "An implantable versatile electrode-driving asic for chronic epidural stimulation in rats," *IEEE Trans. Biomed. Circuits Syst.*, no. 3, pp. 387–400, June 2015.

[6] K. F. Winter, R. Hartmann, and R. Klinke, "A stimulator with wireless power and signal transmission for implantation in animal experiments and other applications," *J. Neurosci. Methods*, vol. 79, no. 1, pp. 79–85, 1998.

[7] R. G. Dennis, D. E. Dow, and J. A. Faulkner, "An implantable device for stimulation of denervated muscles in rats," *Med. Eng. Phys.*, vol. 25, no. 3, pp. 239–253, 2003.

[8] R. E. Millard and R. K. Shepherd, "A fully implantable stimulator for use in small laboratory animals," *J. Neurosci. Methods*, vol. 166, no. 2, pp. 168–177, 2007.

[9] D. Harnack, W. Meissner, R. Paulat, H. Hilgenfeld, W. D. Müller, C. Winter, R. Morgenstern, and A. Kupsch, "Continuous high-frequency stimulation in freely moving rats: Development of an implantable microstimulation system," *J. Neurosci. Methods*, vol. 167, no. 2, pp. 278–291, 2008.

[10] S. K. Arfin, M. A. Long, M. S. Fee, and R. Sarpeshkar, "Wireless neural stimulation in freely behaving small animals." *J. Neurophysiol.*, vol. 102, no. 1, pp. 598–605, 2009.

[11] S. Ethier and M. Sawan, "Exponential Current Pulse Generation for Efficient Very High-Impedance Multisite Stimulation," *Sci. Technol.*, vol. 5, no. 1, pp. 30–38, 2011.

[12] R. de Haas, R. Struikmans, G. van der Plasse, L. van Kerkhof, J. H. Brakkee, M. J. H. Kas, and H. G. M. Westenberg, "Wireless implantable micro-stimulation device for high frequency bilateral deep brain stimulation in freely moving mice," *J. Neurosci. Methods*, vol. 209, no. 1, pp. 113–119, 2012.

[13] D. W. J. Perry, D. B. Grayden, R. K. Shepherd, and J. B. Fallon, "A fully implantable rodent neural stimulator," *J. Neural Eng.*, vol. 9, no. 1, p. 014001, feb 2012.

[14] S. G. Ewing, B. Porr, J. Riddell, C. Winter, and A. A. Grace, "SaBer DBS: A fully programmable, rechargeable, bilateral, charge-balanced preclinical microstimulator for long-term neural stimulation," *J. Neurosci. Methods*, vol. 213, no. 2, pp. 228–235, 2013.

[15] H. Xu, E. Noorsal, K. Sooksood, J. Becker, and M. Ortmanns, "A multichannel neurostimulator with transcutaneous closed-loop power control and self-adaptive supply," *ESSCIRC*, pp. 309–312, 2012.

[16] S. K. Arfin and R. Sarpeshkar, "An energy-efficient, adiabatic electrode stimulator with inductive energy recycling and feedback current regulation," *IEEE Trans. Biomed. Circuits Syst.*, vol. 6, no. 1, pp. 1–14, 2012.